Application of an inverse scheme for acoustic source localization

Stefan Gombots[1], Manfred Kaltenbacher[2], Barbara Kaltenbacher[3]

[1] *Institue of Mechanics and Mechatronics, 1060 Vienna, Austria, Email: stefan.gombots@tuwien.ac.at*

[2] *Institue of Mechanics and Mechatronics, 1060 Vienna, Austria, Email: manfred.kaltenbacher@tuwien.ac.at*

[3] *Institute of Applied Analysis, 9020 Klagenfurt, Austria, Email: barbara.kaltenbacher@aau.at*

Abstract

Acoustic source localization techniques in combination with microphone array measurements have become an important tool for noise reduction tasks. Furthermore, these techniques are used for failure diagnosis and condition monitoring. A common technique for this purpose is acoustic beamforming, which can be used to determine the source locations and source distribution. Main restrictions using this method are given by the description of the transfer function between source and microphone signal using Green's function for free radiation and by using simplified source models. Hence, reflecting (or partially reflecting) surfaces are not really considered, and the method of using mirror sources is quite limited. To overcome these limitations, the corresponding partial differential equation in the frequency domain (Helmholtz equation) will be solved by applying the Finite Element Method (FEM) with the actual boundary conditions as given in the measurement setup. Next, the inverse problem of matching measured (microphone signals) and simulated pressure is solved to recover the source locations. The applicability of the inverse scheme to a real world situation and the additional benefit compared to acoustic beamforming will be demonstrated.

Introduction

The knowledge about the position and distribution of dominant sound sources is necessary for taking actions in noise reduction. Hereby, acoustic source localization techniques have become an important tool to locate and quantify the acoustic sources. A common method for acoustic source localization is beamforming using microphone array measurements. It is used to determine the source location and distribution, and to quantify the source strength. The results are given in so called source maps, who visualize the source distribution and strength. The fundamental processing method, Frequency Domain Beamforming (FDBF) [1] is a robust and fast technique. Here, the source map σ is computed by

$$\sigma(\boldsymbol{g}) = \sqrt{\frac{\boldsymbol{g}^{\mathrm{H}}\boldsymbol{C}\boldsymbol{g}}{\boldsymbol{g}\boldsymbol{g}^{\mathrm{H}}}} \tag{1}$$

with $\boldsymbol{g}$ the Green's function for free radiation and $\boldsymbol{C}$ the cross spectral matrix of the microphone signals. The $^{\mathrm{H}}$ denotes the hermitian operation (complex conjugation and transposition). The resolution and dynamic of FDBF is limited. The limitation of the resolution and dynamic is caused by the Point Spread Function of the microphone array, which is the convolution of the spatial impulse response of the array with a single point source. To overcome these drawbacks, one can use deconvolution techniques, e.g. DAMAS [2], Clean-SC [3] etc., which convert the raw FDBF source map (Eq. (1)) into a deconvoluted source map, resulting in higher resolution and dynamic range. However, one has to deal with some restrictions. First, most beamforming algorithms models the acoustic source by monopols, so that the transfer function between source and microphone is given by Green's function for free radiation. Hence, reflecting or partially reflecting surfaces are not really considerable, and the method of mirror sources is quite limited. Further, the phase information of the acoustic sources is lost in the source map and the beamforming methods doesn't perform well at low-frequencies. Next, we will present the approach of our inverse scheme for acoustic source localization.

Inverse scheme

To overcome these limitations, we propose an inverse scheme based on a constrained minimization problem. In the provided inverse scheme a cost functional is minimized such that the physical model with source terms is fulfilled. Assuming that the original geometry of the setup including the boundary conditions and the Fourier-transformed acoustic pressure signals $p_i^{\mathrm{ms}}(\omega)$ (ω being the angular frequency, $i = 1, \ldots, M$) at the microphone positions $\boldsymbol{x}_i$ are given, the physical model is represented by the Helmholtz equation. Here, we consider the following generalized form of the Helmholtz equation in $\Omega = \Omega_{\mathrm{acou}} \cup \Omega_{\mathrm{damp}}$

$$\boldsymbol{\nabla} \cdot \frac{1}{\rho}\boldsymbol{\nabla} p + \frac{\omega^2}{K} p = \sigma^{\mathrm{in}} \text{ in } \Omega, \tag{2}$$

with the searched for interior acoustic sources $\sigma^{\mathrm{in}}(\boldsymbol{x})$ in the domain $\Omega_{\mathrm{sc}} \subset \Omega_{\mathrm{acou}}$ and

$$\rho(\boldsymbol{x}) = \begin{cases} \tilde{\rho}_{\mathrm{eff}} & \text{in } \Omega_{\mathrm{damp}} \\ \rho_0 & \text{in } \Omega_{\mathrm{acou}} \end{cases}$$

$$K(\boldsymbol{x}) = \begin{cases} \tilde{K}_{\mathrm{eff}} & \text{in } \Omega_{\mathrm{damp}} \\ c^2\rho_0 & \text{in } \Omega_{\mathrm{acou}} \end{cases}.$$

Herewith, absorbers can be considered as a layer of an equivalent complex fluid having a frequency-dependent effective density $\tilde{\rho}_{\mathrm{eff}}$ and bulk modulus $\tilde{K}_{\mathrm{eff}}$. With this formulation the absorption properties of the boundary

can be adjusted to a certain absorption coefficient. Furthermore, sound sources on the surface of an obstacle are modelled by

$$\boldsymbol{n} \cdot \nabla p = \sigma^{\mathrm{bd}} \quad \text{on } \partial\Omega_{\mathrm{obstacle}}. \tag{3}$$

Since the identification is done separately for each frequency ω, the dependence on ω was neglected in the notation. Now, the considered inverse problem is to reconstruct σ^{in} and/or σ^{bd} from pressure measurements

$$p_i^{\mathrm{ms}} = p(\boldsymbol{x}_i)\,, \quad i = 1, \ldots, M \tag{4}$$

at the microphone positions $\boldsymbol{x}_1, \ldots, \boldsymbol{x}_M$. For the acoustic sources the following ansatz is made

$$\sigma^{\mathrm{in}} + \sigma^{\mathrm{bd}} = \sum_{j=1}^{N} a_j e^{i\varphi_j} \delta_{\boldsymbol{x}_j} \tag{5}$$

with the searched for amplitudes $a_1, a_2, ..., a_N \in \mathbb{R}$ and phases $\varphi_1, \varphi_2, ..., \varphi_N \in [-\pi/2, \pi/2]$. Here, N denotes the number of possible sources and $\delta_{\boldsymbol{x}_j}$ the delta function at position $\boldsymbol{x}_j$.

Optimization based source identification

The fitting of the parameters by means of Tikhonov regularization amounts to solving the following constrained optimization problem

$$\min_{p \in U, a \in \mathbb{R}^N, \varphi \in [-\frac{\pi}{2}, \frac{\pi}{2}]^N} J(p, a, \varphi) \;:\; \text{Eq.(2) is fulfilled} \tag{6}$$

where $a = (a_1, \ldots, a_N)$, $\varphi = (\varphi_1, \ldots, \varphi_N)$ and

$$\begin{aligned} J(p, a, \varphi) \quad = \quad & \frac{1}{2} \sum_{i=1}^{M} |p(\boldsymbol{x}_i) - p_i^{\mathrm{ms}}|^2 \\ & + \alpha \sum_{j=1}^{N} \left| a_j \right|^q + \beta \sum_{j=1}^{N} \varphi_j^2 \,. \end{aligned} \tag{7}$$

Sparsity of the reconstruction is desired to pick the few true source locations from a large number of the N trial sources. By choosing $q \in (1, 2]$ close to one one can enhance sparsity. The regularization parameters α, β are chosen according to the sequential discrepancy principle [6]

$$\beta = \alpha = \alpha_0 2^{-m} \tag{8}$$

with m the smallest exponent such that following inequality

$$\sqrt{\sum_{i=1}^{M} \left(p(\boldsymbol{x}_i) - p_{\mathrm{m}i}\right)^2} \leq \varepsilon$$

is fulfilled, with ε the measurement error. Further details of the inverse scheme can be found in [4] [5].

Results

To demonstrate the applicability of the presented inverse scheme, a numerical example was used. The computational setup (see Fig. 1) is based on a room at TU Wien. In the numerical example, the identification of the sources will be done in a source region Ω_{sc} (case I) and on a surface $\partial\Omega_{\mathrm{obstacle}}$ (case II). In case II a circular membrane was used as acoustic source, wherein the normal velocity was prescribed. In case I a monopol source 0.1 m bellow the midpoint of the membrane was used. For both cases the frequency is 500 Hz.

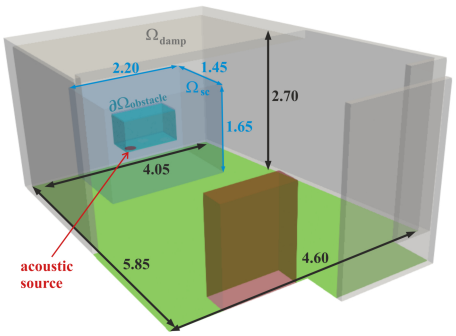

Figure 1: Computational setup based an a room at TU Wien (dimensions in m). The dimension of the obstacle $\partial\Omega_{\mathrm{obstacle}}$ is $0.5 \times 1 \times 0.5$ m and of the red box $0.4 \times 1.2 \times 1.5$ m.

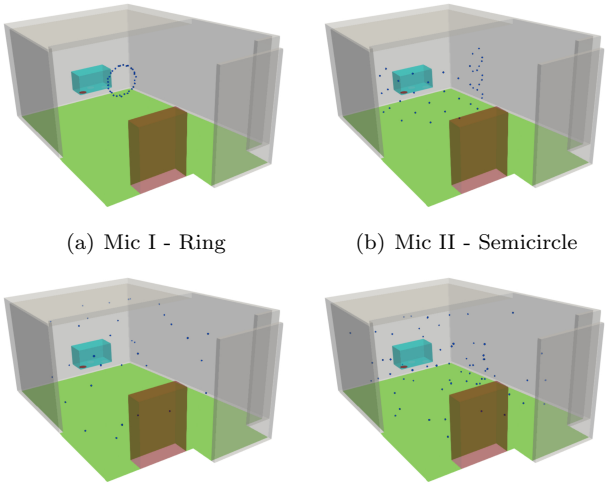

(a) Mic I - Ring (b) Mic II - Semicircle

(c) Mic III - Random I (d) Mic IV - Random II

Figure 2: Different microphone arrangements.

The room is partially lined with porous absorbers on the walls (denoted by Ω_{damp}). The absorber (BASOPLAN100 [7]) is modelled by an equivalent complex fluid with $\tilde{\rho}_{\mathrm{eff}} = 2.78 - 1.39\mathrm{j}$ and $\tilde{K}_{\mathrm{eff}} = 100000 + 10000\mathrm{j}$ fitted from an impedance tube measurement of the absorber (absorption coefficient $\alpha = 0.95$ at 500 Hz). All other surfaces were modelled fully reflective (sound hard). The speed of sound c is assumed to be 343 m/s.

In our investigations we use four different microphone array arrangements which can bee seen in Fig. 2. The first arrangement Mic I (Fig. 2(a)) uses 32 microphones on a ring with diameter of 1 m. It is a classical array for acoustic beamforming where the microphones are placed just on a plane. The next configuration Mic II (Fig. 2(a)) consists of 38 microphones. Here, the microphones are on a semicircle (radius of 1.4 m) around the obstacle. At Mic III (Fig. 2(c)) and Mic IV (Fig. 2(d)) the 32 respectively 64 microphones are randomly distributed in the room. To simulate realistic measured pressure values

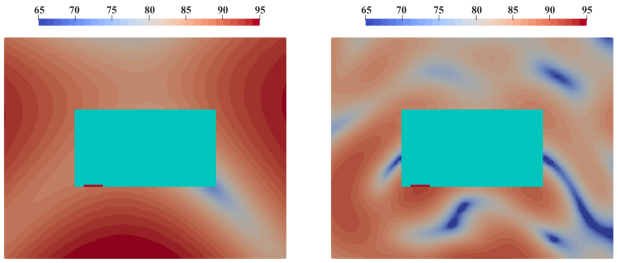

(a) Mic I - Ring (b) Mic IV - Random II

Figure 3: Beamforming results with different microphone arrangements, sound source level L_σ.

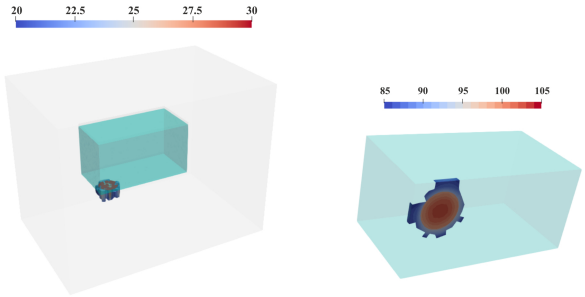

(a) Case I - L_σ (b) Case II - L_v

Figure 4: Original acoustic sources.

at the microphone positions, the computation was done on a much finer grid than for the identification of the acoustic sources. The fine grid had about 4.3 million degrees of freedom whereas the grid for identification has about 0.7 million. Additionally random noise was added to the simulated data to obtain a signal-to-noise ratio of 10 dB. As mentioned before the absorbers on the walls were represented by a complex fluid. Moreover, the normal velocity of a loudspeaker was measured and used in the computation. Finally, the microphone positions in the computation and identification differ from each other in the range of ± 5 cm.

First, we use Mic I and FDBF (Eq. (1)) to identify the sources in the room. Hereby, the setting of 2D Beamforming has been used. Therefore, a scanning area was put through the obstacle parallel to the ring array cutting the obstacle in the middle. Further, configuration Mic IV was also used for identification with beamforming. The results of FDBF can be seen in Fig. 3. Here, both microphone arrangements don't provide good results, there are a lot of fictitious sources in the source maps. The reverberation time in the interesting one-third octave band of 500 Hz is about 180 ms and was determined through measurement with an impulse source. This led beamforming perform quite bad and also the relatively low-frequency of 500 Hz contributes to the worse result. Clean SC also identifies the source on totally wrong position (in the best case 0.45 m away from the true position).

For the identification of the acoustic sources with the inverse scheme, we set the starting values of the regularization parameters to $\alpha = 0.125$ and $\beta = 0.125$. The maximum number m for the reduction of the regularization parameters were set to 15. To achieve sparsity of the reconstruction the exponent q was chosen to be 1.1. There were 46593 possible sources for case I and 4250 for case II. The implemented optimization based parameter identification algorithm is based on a gradient method with Armijo line search exploring the adjoint method to efficiently obtain the gradient of the objective function (Eq. 7). Hence, the computation time does not depend on the number of trail sources N and the number of microphones M. The total elapsed CPU time (stand-alone PC with an Intel Xeon E5-2697A, 2.60 GHz processor) for the identification of the acoustic sources was about 320 hours. Thereby, all 15 steps for the reduction of α and β have been performed.

Next, the results of the reconstruction using the inverse scheme for the different microphone arrangements will be given. First, the original acoustic sources used for simulating the measured pressure values are shown in Fig. 4. For case I the source level

$$L_\sigma = 20 \log \left(\frac{\sigma}{2 \cdot 10^{-5}\ \mathrm{N/m}} \right) \tag{9}$$

is shown and for case II the particle velocity level

$$L_v = 20 \log \left(\frac{v}{5 \cdot 10^{-8}\ \mathrm{m/s}} \right). \tag{10}$$

Case I (searching in Ω_{sc})

The results of the identification in the source region Ω_{sc} can be seen in Fig. 5. As one can see, the original source distribution (Fig. 4(a)) was reconstructed for Mic II, Mic III and Mic IV quite good. The best result according the amplitude can be achieved by Mic IV whereas Mic I performs worst.

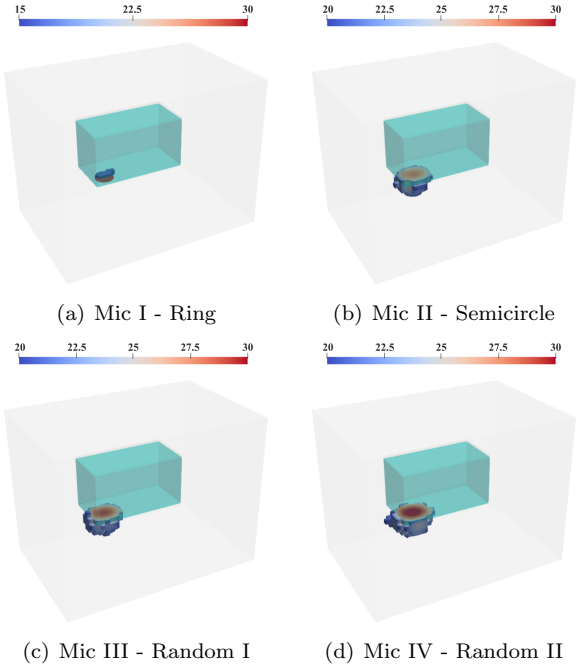

(a) Mic I - Ring (b) Mic II - Semicircle

(c) Mic III - Random I (d) Mic IV - Random II

Figure 5: Reconstruction results of case I for the different microphone arrangements (L_σ is shown).

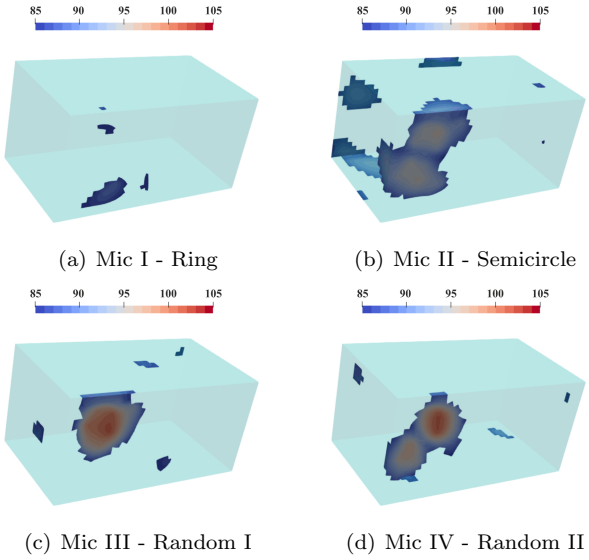

(a) Mic I - Ring (b) Mic II - Semicircle

(c) Mic III - Random I (d) Mic IV - Random II

Figure 6: Reconstruction results of case II for the different microphone arrangements (L_v is shown).

Case II (searching on $\partial\Omega_{\text{obstacle}}$)

Next, we are looking at the reconstruction results when identifying the sources on the surface $\partial\Omega_{\text{obstacle}}$, see Fig. 6. Comparing them with the original acoustic normal velocity level (Fig. 4(b)) one can clearly see that arrangement Mic I (Fig. 6(a)) fails. Mic II (Fig. 6(b)) and Mic IV (Fig. 2(d)) identifies two sources whereby at Mic II are more source artefacts than at Mic IV. Here configuration Mic III provides the best results regarding source distribution and amplitude.
In a next step we use the identified sources of Fig. 6(c) to perform a sound field computation giving the sound field showed in Fig. 7(b). Here, a really good agreement with the original sound field can be achieved, see Fig. 7(a).

Conclusion and Outlook

Results of identifying acoustic sources in a source region and on a surface by the inverse scheme were presented. The identification of the sources was done in a relatively small room at a low-frequency. At such conditions beamforming won't perform quite good. Hereby, a main restriction is given through the Green's function for free radiation. The simulation-based sound source identification allowed us to consider the actual boundary conditions as given in the measurement setup. Moreover, the numerical results showed the potential of the inverse method and the applicability in the low-frequency range and also the calculation of the sound field based on the identified sources provides really good results. Further, it has been shown that the positioning of the microphones have a significant impact on the identification result leading to the question of optimal microphone positions for the identification. In a next step, we will do real measurements in the simulated room and apply the inverse scheme to identify the sound sources.

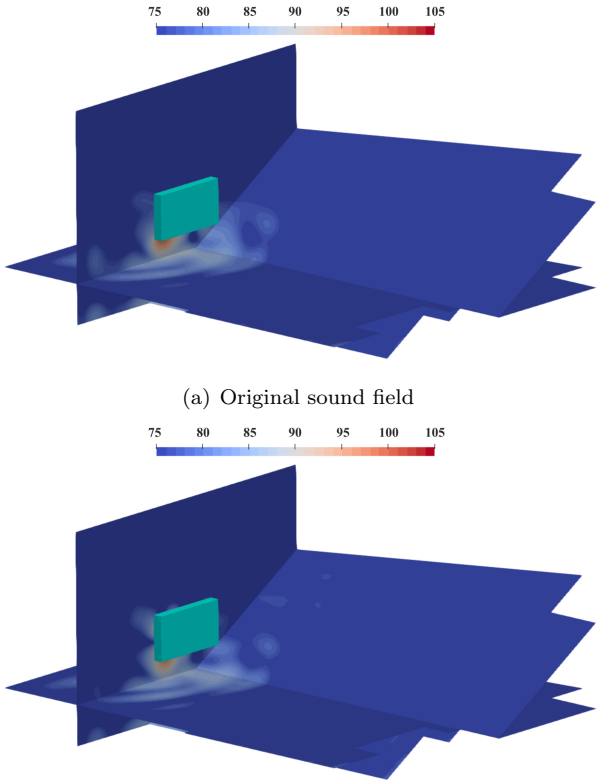

(a) Original sound field

(b) Reconstructed sound field (Mic IV)

Figure 7: Computed sound pressure level.

References

[1] T. J. Mueller: Aeroacoustic measurements. Springer-Verlag Berlin Heidelberg, 2002.

[2] T. F. Brooks, W. M. Humphreys: A deconvolution approach for the mapping of acoustic sources (damas) determined from phased microphone arrays. Journal of Sound and Vibration, 294 (2006), 856-879

[3] P. Sijtsma: CLEAN based on spatial source coherence. International Journal of Aeroacoustics, Vol. 6, 4 (2007), 357-374

[4] Kaltenbacher, M. et al.: Inverse Scheme for Acoustic Source Localization using Microphone Measurements and Finite Element Simulations. Acta Acustica united with Acustica 90 (2018), 647-656

[5] Gombots, S. et al.: Inverse scheme for acoustic source localization in 3D. Euronoise 2018 Crete, ISSN: 2226-5147 (2018), 2597-2602

[6] S. W. Anzengruber, B. Hofmann, P. Mathé: Regularization properties of the sequential discrepancy principle for Tikhonov regularization in Banach spaces. Applicable Analysis, 93 (2014), 1382-1400

[7] Sonatech, URL: `https://www.sonatech.de/files/pdf/Baso-Schaumstoffe/Baso-Plan/Schallabsorber-Datenblatt_Baso_Plan_G.pdf?xoid=7r54dn82166ka6e70m26hkikd0`